ORIGINAL
2/23/99 Log 3/24/99

HUNTINGTON MEDICAL RESEARCH INSTITUTES
NEUROLOGICAL RESEARCH LABORATORY
734 Fairmount Avenue
Pasadena, California 91105

Contract No. N01-NS-8-2399
Quarterly Progress Report
Oct 1, 1998 - Dec 31, 1998
Report No.1

"Microstimulation of the Lumbosacral Spinal Cord"

Douglas B. McCreery, Ph. D.
Albert S. Lossinsky, Ph.D.
Leo Bullara, B.A.
Ted G. F. Yuen, Ph,D.
William F. Agnew, Ph.D.

SUMMARY

We present the results from two animals (sp99 and sp100). One array containing 3 activated iridium microelectrodes was implanted chronically into the S_2 spinal cord of each animal. Twenty-four days after implantation, the cats were anesthetized with Propofol and one or two of the microelectrodes were pulsed continuously for 12 hours on 2 successive days, using charge-balanced, cathodic-first controlled-current pulses, 150 μs/phase in duration. The pulse rate was 50 Hz and the pulse amplitude was 50 μA (7.5 nC/phase).

The best histologic data were obtained from cat sp100, in which the electrodes were close to the intended target in the intermediolateral cell column. The stimulation regimen produced no tissue injury that could be attributed to the electrical stimulation. There was a small amount of tissue scarring that may have occurred during insertion of the electrodes, and/or during subsequent slight movement of the electrodes. Overall, the arrays appear to have been very stable. Although the electrodes had been implanted at a fairly high velocity (~1m/sec), the histologic evaluation, and the videotapes taken at the time of implantation indicated that the spinal cord had dimpled and rotated slightly during the insertion process. One possible solution to this problem will be to increase the speed at which the electrodes are inserted.

We have been developing immunohistochemical techniques which will help to elucidate the tissue response to the chronically implanted microelectrodes and to the electrical stimulation. These include protocols for identifying the leukocytes according to their specific surface antigens (CD antigens). Also of interest is a cell adhesion molecule (ICAM-1) that occurs during neovascularization and also is associated with changes in the blood-brain barrier (BBB) and blood-spinal cord barrier (BSB). We also stained for the glial-associated filamentous protein (GFAP), a commonly-used marker for normal and reactive astrocytes. Finally, we are developing protocols for the enzyme nitrous oxide synthase (NOS), and the growth associated phosphoprotein (GAP-43), two neuronal markers. The initial results for immunostaining for GFAP, NOS, GAP-43, ICAM-1 and CD13 were encouraging, in spite of the technical difficulties inherent in

working with feline tissues perfused with a fixative containing a high concentration of glutaraldehyde.

INTRODUCTION

One of the objectives of this contract is to develop electrode arrays suitable for chronic implantation into nuclei in the feline sacral spinal cord that control urogenital function. A second objective is to use these chronically-implanted arrays to determine protocols for safe and effective stimulation of the neurons in these nuclei. Our primary target is the intermediolateral cell column of the S_2 cord, which contains the preganglionic parasympathetic neurons that innervate the detrusor muscle of the urinary bladder.

We have been examining the effects of electrode implantation, electrode residence, and the subsequent effects of the electrical stimulation, using conventional light-microscopy (paraffin-embedded tissue sections stained with Nissl or with Hematoxylin and Eosin, H&E). Under the workscope of this contract and of a related contract (NO1-NS-8-2388), we have been developing immunohistochemical techniques which will help to elucidate the tissue response to the chronically implanted microelectrodes and to the electrical stimulation. These include protocols for identifying the leukocytes which aggregate around the electrode shafts (and around the tips of pulsed electrodes) according to their surface antigens (CD antigens). The leukocytic subsets of interest that may be expected to play a role in inflammatory responses include the T- and B-lymphocytes, granulocytes such as neutrophils, (and also eosinophils and basophils), as well as mononuclear cells and macrophages. Also of interest is a cell adhesion molecule (ICAM-1) that occurs during neovascularization and also is associated with changes in the BBB and BSB. We also stained for the glial-associated filamentous protein (GFAP), a commonly used marker for normal and reactive astrocytes. We are developing protocols for the two neuronal markers, Nitrous Oxide Synthase (NOS), and for the neuronal Growth-Associated Phosphoprotein (GAP-43). Nitric oxide has been implicated in the "neurogenic inflammatory response" and some preliminary results indicate that it may help to mediate stimulation-induced neuronal injury. Immunohistochemical studies of CD13, an antigenic marker for neutrophils, were also performed.

In the last year, we changed our tissue embedding protocol from epoxy-type

plastic embedding to paraffin embedding for light microscopic analysis, in order to expedite the processing of the histologic material. Although this approach prevents us from conducting fine structural studies, we will be able to schedule specific animals for plastic embedding and subsequent electron microscopic analysis. We also present pilot immunohistochemical data from tissue embedded in the water-soluble embedding medium glycol methacrylate. Glycol methacrylate can be sectioned more thinly than can paraffin, and allows resolution of structural detail similar to that which is attainable with epoxy-type plastics. It also permits the localization of cell-associated antigenic proteins by light and electron microscopy.

Dr. Lossinsky's previous experiences with rodent models of experimental autoimmune disease served as a point of departure for our cat studies. As positive controls for leucocytes, we used the cat spleen, and also subcutaneous tissue near subcutaneous cables when we observed a local skin infection. When our techniques had been developed to the point where we could repeatedly demonstrate differential staining of the various CD antigens in the cat spleen or subcutaneous tissue, we then began an evaluation of sacral spinal cord sections containing the electrode tracks.

There have been few publications pertaining to immunohistochemical techniques for demonstrating the various leukocyte antigens or adhesion molecules in feline CNS tissues. Thus, much of the information submitted herein has previously not been published. It is hoped that these additional studies will offer new insights into cellular changes that may occur during electrical stimulation in the cat sacral spinal cord.

METHODS

Microelectrode arrays and surgical Procedures.

The microelectrode arrays contain 3 activated iridium microelectrodes, staggered in length (1.4, 1.5 and 1.6 mm). The microelectrodes are 500 μm apart, and extend from an epoxy matrix 2 mm in length and approximately 0.75 mm in width. The microelectrodes themselves are 35 μm in diameter and are insulated with Epoxylite 6001 electrode varnish. The tips are fairly blunt (radius of curvature of 1.5 to 2 μm).

Our objective is for the tips to be sufficiently blunt so as not to injure the microvasculature of the spinal cord, yet sharp enough to minimize dimpling of the pia during insertion. The arrays have cables composed of 3 pure platinum wire, each 50 μm in diameter and insulated with Teflon. These cable are very flexible, and do not tend to dislodge the arrays after they have been implanted.

Two adult cats (sp99, sp100) were anesthetized with a mixture of nitrous oxide and Halothane. The spinal cord was exposed from the L_6 to S_3 root level with a standard dorsal laminectomy. The dorsal spinal process anterior to the laminectomy was secured with a vertebral clamp. In both cats, the target was the lateral cell column of the preganglionic, parasympathetic nucleus, which innervates the bladder detrusor muscle. The S_2 level of the spinal cord was located by stimulating electrically the dermatome innervated by the S_2 root (the perigenital region) as a recording electrode was moved rostro-caudally over the dorsal surface of the cord. The rostral-caudal position at which the maximum evoked response is recorded indicates the middle of the S_2 segment of the cord. A longitudinal incision was made through the dura at this level. The arachnoid was then dissected from the dorsal roots.

Only one array of three microelectrodes was implanted into each animal. In each animal, a second array was damaged while unpacking it from its transport holder. (We have subsequently increased the diameter of the iridium microelectrode shafts to 50 μm, in order to minimize the chance that they will be damaged during handing and insertion into the cord). The arrays were implanted with the aid of a modified tool that had been designed to implant microelectrode arrays into the human cochlear nucleus. The instrument was mounted on the spinal apparatus, so that it is oriented vertically, and is mechanically stable. With this instrument, the electrodes can be inserted at a specified velocity. They were inserted vertically into the right side of the S_2 segment of the cord, through the dorsal root entry zone, at a velocity of slightly less than 1 m/sec. In cat sp99, the array was implanted as far lateral as possible (1.0 mm to the right of the cord's midline). The subsequent histologic analysis revealed that the array was much too far lateral, at the extreme outer edge of the lateral white columns. Therefore, in cat sp100, the array was implanted 0.75 mm lateral of the cord's midline.

After implanting the array, the dura was closed very loosely with two 7-0 polyfilament sutures (which also lie over the array cables about 3 mm from the matrices, and helped to keep the arrays from lifting out of the cord). The cables were recurred back to the caudal end of the dural incision, and sutured to the dura. The recording electrode was inserted through the dura, to lie along the ventral roots on the right side, and the reference electrode was placed in the epidural space. The loose dura closure was then covered with a patch of fascia resected from the para-spinal muscles. The para-spinal muscles were approximated with sutures, and the skin closed with sutures.

Twenty four days after implanting the arrays, the cats were anesthetized with Propofol and one (sp100) or two (sp99) microelectrodes were pulsed for 12 hours on each of two successive days. The pulse amplitude was 50 μA. The electrodes were pulsed for 12 hours per day on 2 successive days. In cat sp99, the two adjacent microelectrodes were pulsed simultaneously, using cathodic-first, controlled-current pulses, 150 μs/phase in duration, at rate of 50 Hz.

Histology.

Immediately after the end of the second day of stimulation, the animals were deeply anesthetized with pentobarbital and perfused through the ascending aorta with 4 L ½ strength Karnovsky's Fixative in 0.1 M sodium phosphate buffer at pH: 7.3 (½ K) following blood washout using heparinized PBS. The sacral spinal cord was resected and the capsule of connective tissue covering the elongated array matrices was removed with the arrays *in situ.* A length of suture was then affixed to the surface of the matrix using rapid adhesion glue. After five minutes, the glue is dry and the suture is used to draw the array straight up and out of the spinal cord. The arrays were then placed into glycerol for storage. Spinal roots were identified to determine the exact level of the arrays. The tissue blocks were marked with India ink on their cut rostral surface and embedded in paraffin. Some brain and spinal cord tissues obtained from previous animals and stored in buffer were embedded in the water-soluble embedding medium glycol methacrylate for subsequent pilot immunohistochemical studies. The paraffin-embedded tissue was cut at a thickness of 8 μm and stained with hematoxylin

and eosin (H&E) or with Toluidine blue (Nissl).

Immunohistochemistry.

We applied standard immunohistochemical methods to study possible changes in membrane-associated cellular proteins that may be expressed during electrical stimulation or inflammation. The following proteins were examined: GFAP, NOS, GAP-43, ICAM-1 and CD-13. We used spinal cord tissues from sp99 and sp100 for GFAP, NOS and ICAM-1. GAP-43 was studied in cat brain taken from a previous animal used under another NIH contract. CD4, CD8, and CD13 were examined in spleen from sp86, an animal that was fixed with buffered 4% formalin containing only 0.1% glutaraldehyde (immunofixative = IF) as a positive control tissue, or from spinal cord from cat sp98, which was fixed with ½ K.

Glass slides with 8 μm paraffin sections containing, or adjacent to, electrode tracks were selected for immunohistochemical incubations. The selection process in this pilot experiment was conducted blindly, with respect to which electrodes were pulsed or unpulsed. The tissue sections were rehydrated, blocked with either DAKO or ZYMED protein blocking solution and treated with hydrogen peroxidase to remove endogenous peroxidase activity. An antigen retrieval method was also applied using brief microwave heating and citrate buffer, at pH 7.2. After washing with PBS, the tissue sections were incubated with primary and secondary antibodies, followed by expression of the chromogen using the peroxidase-diaminobenzidine (HRP-DAB) method (Birchall, 1996). A disadvantage of this methods is that the peroxidase reaction product appears as a brown color on a blue counterstained background, which can be discerned only by direct observation or in a color photograph. Some antigens were expressed using the immunogold label with silver enhancement (Lucocq and Roth, 1985). The latter method that may allow better localization of the antigen because the reaction product results in a dark precipitate. This approach has merit when reporting our finding in QPRs and in publication in which color prints are not practical.

After incubations, all sections were counter-stained with a weak solution of hematoxylin. Negative controls were tissues obtained from adjacent spinal cord blocks,

either rostral or caudal to the block containing the electrodes. Other negative control tissue included cerebral cortex obtained from previous cat experiments. The control sections were incubated in a manner similar to the experimental slides, but without the addition of primary antibodies.

We also conducted immunohistochemical studies of brain and spinal cord tissues embedded in the water-soluble embedding medium glycol methacrylate. Our goal was to obtain immunohistochemical staining in tissue sections that are thinner than is possible with paraffin, thus allowing improved visualization of structural details. Two μm sections were cut from one tissue block adjacent to the block containing the electrodes and processed for the detection of NOS, according to the method prescribed for methyl methacrylate resin (Blyth et al., 1997). The resin was then removed with xylene. The protocol followed for these sections was essentially identical to that which was performed on the paraffin sections. After protein blocking and application of anti-NOS primary and secondary antibodies, treatment with HRP-DAB yielded a brown reaction product visible by light microscopy. Negative controls for this series were similar to those in the paraffin-imbedded series, as described above. We observed that immersion in 1% osmium tetroxide solution for 2 seconds intensified the reaction products for both DAB and the silver enhancement techniques (Hawkins, 1999; Hawkins et al., 1996). Glycol methacrylate sections were stained with either hematoxylin or with toluidine blue.

RESULTS

Histology.

Autopsy examinations of sp99 and sp100 revealed that the array matrices were located near the dorsal root entry zones in the S_2 regions of the spinal cord. The cord level was determined from the insertion points of the dorsal roots of identified spinal nerves (Figures 1-3). In sp99, the electrodes were angled laterally into the lateral white columns, and they produced a slight bulge on the surface of the lateral white column (Figure 1). The array matrix had induced pronounced compression of the cord's dorsal surface (Figure 4).

Figure 4 shows a histologic section through the S_2 spinal cord of cat sp99. In this animal, electrode #1 and 2# were pulsed, and electrodes #3 was not pulsed. Although the electrodes had been implanted with inserter oriented vertically, the electrodes were angled sharply away from the dorsal-ventral axis of the cord. Analysis of the video of the insertion procedure revealed that this deviation was caused by rotation of the sacral cord during insertion of the array. This not only caused the array to miss its target in the intermediolateral gray matter, but also inflicted injury in the lateral white column. There was vascular hyperplasia, gliosis, hemorrhage and an infiltration of a few leukocytes, as well as spongy changes that indicate degeneration of the longitudinally-oriented axons. (Figures 5-7).

In cat sp100, the array was inserted more medially (0.75 mm from the cord's midline), and with better results. The microelectrodes were positioned within the right lateral intermediolateral gray matter, and in the ventrolateral gray (Figure 8). The depth of penetration varied according to the length of each electrode. The electrode tracts were angled slightly away from the dorsal-ventral axis, but much less so than in cat sp100. Analysis of the video of the electrode insertion process revealed some rotation of the cord. This suggests that the speed at which the electrode are inserted should be increased.

In the electrical stimulation study, only electrode #1 in cat sp100 was pulsed. Topically-applied India Ink (used to facilitate orientation and trimming of the spinal cord blocks prior to embedding) appears as an aggregate of opaque particles within the lumen of the electrode track and blood-vessels, and partially obscured the tissue immediately adjacent to the track. We will not use this technique in future animals. However, the ink was confined to the lumen of the track, and we were able to evaluate the neuropil in the 3rd sections, approximately 16 μm lateral to the actual tip site. The neurons in the vicinity of the pulsed tips appear to be normal (Figure 9). We observed neuronal chromatolysis in only two neurons in cat sp100, and these were adjacent to unpulsed electrode # 2 (Figures 10, 11). Thus, the stimulation regimen (12 hours of pulsing on two successive days at 50 Hz, 50 μA, 7.5 nC/phase) produced no detectable tissue injury.

The pattern of the distribution of leukocytes near the pulsed and unpulsed electrode was slightly different. Slightly more small, round lymphocytes and scattered mononuclear cells were localized in the vicinity of the tip of pulsed electrode #1, as well as in the glial capsule surrounding the electrode shaft. These cells were also distributed along the sheaths surrounding the unpulsed electrodes (Figure 10). Granular leukocytes, (presumably phagocytes) were infiltrated into the tissue surrounding the tips of the pulsed as well as the unpulsed electrodes. These had phagocytized cellular debris, probably from cells damaged during electrode insertion (Figure 9, 12).

Immunohistochemistry.

Immunohistochemical results were surprisingly good in spinal cord and brain tissue, in spite of the high concentration of glutaraldehyde in the ½ K fixative. Slides with 4-6 sections from cats sp99 and sp100 were examined after immunostaining, and then reexamined after counter-staining with hematoxylin. The best results were obtained from sp100, in which the electrodes were positioned within the gray matter. In sp99, technical problems prevented adequate visualization of the reaction products.

Results for the immunostaining for GFAP, NOS, ICAM-1 and CD13 from sp100 are presented in figures 13-28. GFAP is a protein in fibrous and protoplasmic astrocytes and in perivascular astrocytic end-foot processes. It is expressed most strongly when the astrocytes are reacting to tissue injury. The immunostain was especially pronounced within the tissue adjacent to the capsule surrounding the shaft of unpulsed electrode #2 (Figures 13-15). In a previous cat (sp86) perfused with IF and employing the immunogold and silver enhancement method, GFAP reaction product was clearly visible in fibrous and protoplasmic astrocytes and in their processes (Figure 16), and also it was heavily expressed in glycol methacrylate-embedded material (Figure 17).

The immunostains for NOS and GAP-43 were localized to neurons (Figures 18-22). The reaction product for NOS stained the neuronal perikarya near the pulsed electrode #1 in cat sp100 (Figure 19). The reaction product also stained the large

motoneurons of the ventral horn, in material embedded in glycol methacrylate (Figure 20). NOS (Figure 21) and GAP-43 (Figure 22) were expressed in the cerebral cortex (positive controls) fixed with either ½ K or with IF.

The reaction product for ICAM-1 was most evident in small blood vessels, (presumably post-capillary venules), and in some activated leukocytes within the electrode's capsular sheath and in the adjacent tissue (Figures 23-25).

We attempted to stain for CD13 in spleen tissue from a cat (sp86) perfused with IF, or from the cervical spinal cord of cat sp98, which was fixed with ½ K. Neutrophils were the only cell type that expressed this antigen (Figure 26). Results for CD4, CD8 and CD20 were not conclusive and have not been included in this QPR. Negative control tissues embedded in either paraffin or glycol methacrylate did not show the reaction product (Figures 27, 28).

DISCUSSION

The histologic findings from cat sp100 is encouraging, since they indicate that our arrays, with platinum cables, are quite stable during at least the first few weeks after implantation. The findings also indicate that the stimulation regimen used in these animals (12 hours of pulsing on two successive days at 50 Hz, 50 μA, 7.5 nC/phase) produced little or no tissue injury. The results from these two cats also indicate that we have not completely resolved how best to implant the arrays. The sacral cord is suspended loosely within the spinal canal and it is easily displaced by slight pressure on its dorsal surface. It also rotates easily about its rostral-caudal axis if the force is applied on either side of its midline. Although our longitudinal arrays of 3 microelectrodes appear to be much more stable than individual microelectrodes, the electrode matrix necessitates implanting the arrays from the cord's dorsal surface, to avoid damage to the dorsal roots. In cat sp99, the array was implanted 1.0 mm lateral to the midline of the S_2 cord, and the histology, and the analysis of the video tapes made during implantation indicate that the cord rotated markedly during the insertion. In cat sp100, the array was implanted slightly more medially (0.75 mm from the midline). There was less rotation of the cord, and the electrode tips were much closer to their

target in the intermediolateral cell column. However, in order for the cord's surface topology to be used as a guide for implanting the electrodes into their very small target, and to minimize tissue injury, the rotation and dimpling of the cord must be reduced to an absolute minimum. One solution will be to increase the speed at which the electrodes are inserted.

Although there is abundant literature detailing immunohistochemical methods for the identification of cellular antigenic markers, there is a paucity of literature describing their use in feline tissues, especially for light microscopy. We applied techniques that have been described for other species, and we used our own experience with murine systems in order to established techniques that would be applicable to our studies in the cat spinal cord. As we expected, there was some antigenic cross-reactivity in the cat tissues to several of the commercially available mouse anti-human monoclonal or polyclonal antibodies, including the anti-ICAM-1 antibody (a gift to our laboratory from Dr. Robert Rothlein, Boehringer Ingelheim Pharmaceutical, INC, Ridgefield, CT). Unfortunately, this was not the case for other antibodies, including those for the leukocyte markers CD4 (helper-inducer cells), CD8 (cytotoxic/suppressor cells) and CD20 (B-lymphocytes). These negative result also may be due to the high glutaraldehyde concentration in the ½ K fixative, or we may require antibodies that will recognize feline moieties on these antigenic proteins. We did demonstrate that the CD13 antigen (a marker for neutrophils) as well as those for GFAP, NOS, GAP-43 and ICAM-1 survived the higher glutaraldehyde concentration.

We devoted considerable effort to developing methods that worked with cat control tissues (eg. spleen and inflamed subcutaneous tissue) prior to applying our new methodologies to our limited and rather precious tissue sections of spinal cord containing the electrode tracks. For the leukocyte studies, the cat spleen served as an important positive tissue control for the spinal cord and other brain tissues.

Using routine H&E histopathology, we have recently shown in the cerebral cortex that leukocytes (mostly lymphocytes) cross the BBB and congregate around the tips of pulsed electrodes. The leukocytes disperse within a short period after stimulation ceases, and presumably return to the blood circulation, and usually do not aggregate

around the unpulsed electrodes (Yuen et al., 1998). We expect that immunohistochemical methods to identify the lymphocyte subsets will yield valuable information related to understanding the mechanisms of this aggregations of inflammatory cells. Having established baseline immunohistochemical protocols using paraffin-embedded feline tissues, we will be able to apply these techniques in the feline spinal cord to determine which leukocyte subset(s) aggregate around the pulsed electrodes.

ICAM-1 is an important ligand for its corresponding integrin molecule LFA-1 on the leukocytic membranes, serving to facilitate leukocytic adhesion and trans-vascular emigration (Lossinsky et al., 1999). It is known that the BBB in the mouse brain is fully healed by the fourth week after trauma (Cancilla et al., 1979; Lossinsky et al, 1981). ICAM-1 is upregulated in the blood vessels when the BBB is open (Lossinsky et al, 1995). ICAM-1 appears to have been upregulated within the neovascularization surrounding the sheath of an unpulsed electrode from cat sp100 (Figures 23 - 25). This suggests that the BSB may not have been completely sealed by 24 days after electrode implantation.

We believe that the pilot studies presented here will serve as a basis for future immunohistochemical studies, as well as immunocytochemical studies at the ultrastructural level. These kinds of studies may offer insights into the response of neurons, glia and vasculature elements, during electrode implantation, their chronic residence in the brain and spinal cord, and during electrical stimulation.

WORK FOR NEXT QUARTER

We have conducted, or have scheduled, the implantation of multiple microelectrode arrays into the spinal cords of 3 cats, and we plan to conduct 3 stimulation experiments in this quarter, to confirm the findings from cat sp100. We will also continue developing new immunohistochemical methods to determine which leukocyte subsets (T-cell, B-cell, etc.) aggregate around the pulsed electrodes.

LITERATURE CITED

Benowitz LI, Routtenberg A (1997). GAP-43: an intrinsic determinant of neuronal development and plasticity. TINS 20:84-91.

Birchall IE (1996). Direct antibody method for formalin fixed, paraffin embedded renal biopsies: A comparison with peroxidase labeled streptavidin/biotin method. J Histotechnol 19:125-129.

Blyth D, Hand NM, Jackson P, Barrans SL, Bradbury RB, Jack AS (1997). Use of methyl methacrylate resin for embedding bone marrow trephine biopsy specimens. J Clin Pathol 50:45-49.

Cancilla PA, Frommes SP, Kahn LE, DeBault LE (1979). Regeneration of cerebral Microvessels. A morphologic and histochemical study after local freeze-injury. Lab Invest 40:74-82.

Duchen LW (1992). General pathology of neurons and neuroglia. In: Greenfield's Neuropathology, eds. Adams JH, Duchen LW, Oxford University Press, New York, 5th ed., pp. 1-68.

Hawkins H (1999). Osmium as an immunostain enhancement. Micros Today 99:21.

Hawkins HK, Entman ML, Zhu JY Youker KA Berens K, Dore M. (1996). Acute inflammatory reaction after myocardial ischemic injury and reperfusion. Development and use of a neutrophil specific antibody. Am J Pathol 148:1957-1969.

Kosaka T, Nagatsu I, Wu J-Y and Hama K: (1986). Use of high concentrations of glutaralhedyde for immunocytochemistry of transmitter-synthesizing enzymes in the central nervous system. Neurosci 18:975-990.

Lossinsky AS, Buttle KF, Pluta R, Wisniewski HM, Mossakowski MJ (1999). Immunoultrastructural expression of intercellular adhesion molecule-1 (ICAM-1/CD54) in endothelial cell vesiculo-tubular structures and vesiculo-vacuolar organelles (VVO) in blood-brain barrier development and injury. Cell Tiss Res 295:77-88.

Lossinsky AS, Mossakowski M J, Pluta R, Wisniewski HM: (1995). Intercellular adhesion molecule-1 (ICAM-I) upregulation in human brain tumors as an expression of increased blood-brain barrier permeability. Brain Pathol 5:339-344.

Lossinsky AS, Vorbrodt AW, Wisniewski HM, Iwanowski L: (1981) Ultracytochemical evidence for endothelial channel-lysosome connections in mouse brain following blood-brain barrier changes. Acta Neuropathol (Berl.) 53:197-202.

Lucocq JM, Roth J: (1985). Colloidal gold silver metallic marker for light microscopic histochemistry. In: Techniques in Immunocytochemistry, eds. Bullock GR, Petrusz P, Academic Press, New York, vol. 13, pp. 203-236.

Maines, MD; Nitric Oxide Synthase: Characterization and Functional Analysis. Academic Press, San Diego, p. xv, 1996.

Yuen TGH, Agnew WF, McCreery DB, Bullara LA (1998). Accumulation of lymphocytes elicited by microstimulation of the cat's cerebral cortex. Abstr. Soc. for Neuroscience 24:659.

Figure 1. Sp99. The angle of entry of these electrodes produced a slight bulge in the lateral column (arrowhead).

Figure 2. Sp100. The surface of the electrode array is shown within the S_2 segment of the spinal cord. Note the dorsal root ganglia for L_6 and L_7.

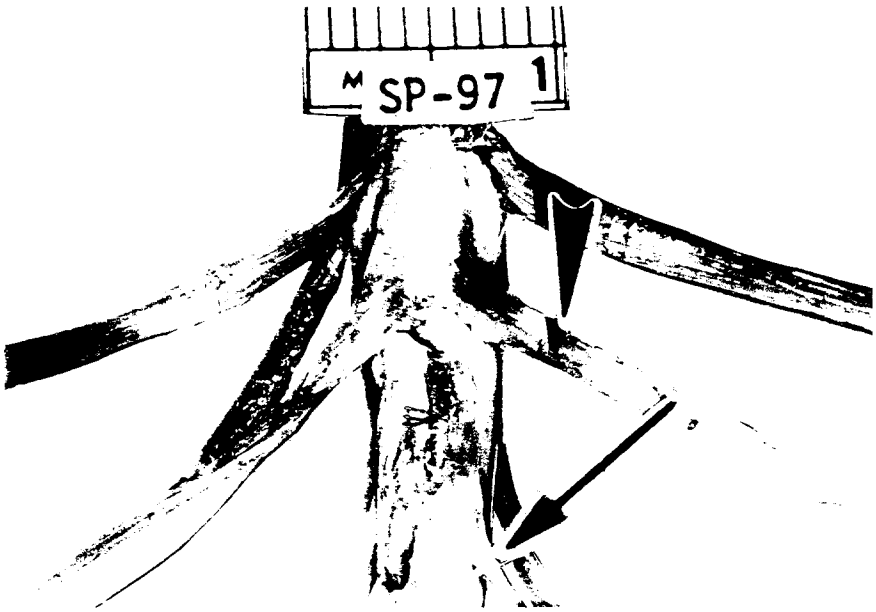

Figure 3. Two three electrodes arrays are shown still implanted in the sacral spinal cord of an animal from a previous experiment (sp97). Dorsal nerves L_7 (arrowhead) and S_1 (arrow) have been separated to demonstrate the neuroanatomical location of the arrays.

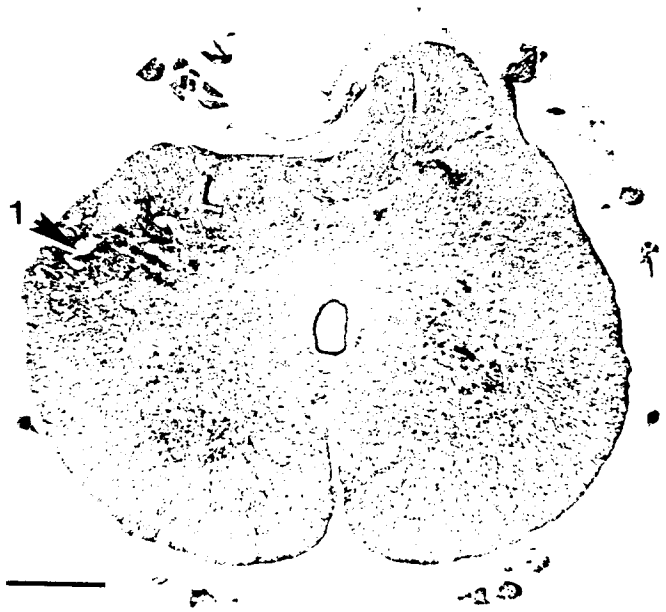

Figure 4, H&E stain. A low-magnification view of the sacral cord of Sp99, showing the compression of the cord's dorsal surface produced by the array matrix. The tip of the pulsed electrode #1 is shown (arrowhead). Bar = 750 µm.

Figure 5. Sp99, H&E stain. Histologic changes produced by both pulsed and unpulsed electrodes include neovascularization (v), reactive astrocytes with gliosis (arrows), and spongy changes within the gray and white matter (s). A few scattered lymphocytes are also observed near the capsular sheath surrounding this pulsed electrode #1 (arrowhead). The lumen of the electrode track is indicated by (*). Bar = 75 µm.

Figure 6. Sp99, H&E stain. Tissue adjacent to pulsed electrode #1. The neurons in the adjacent intermediolateral gray matter appear essentially normal (arrowheads). The lumen of the electrode track is indicated by (*). Bar = 75 µm.

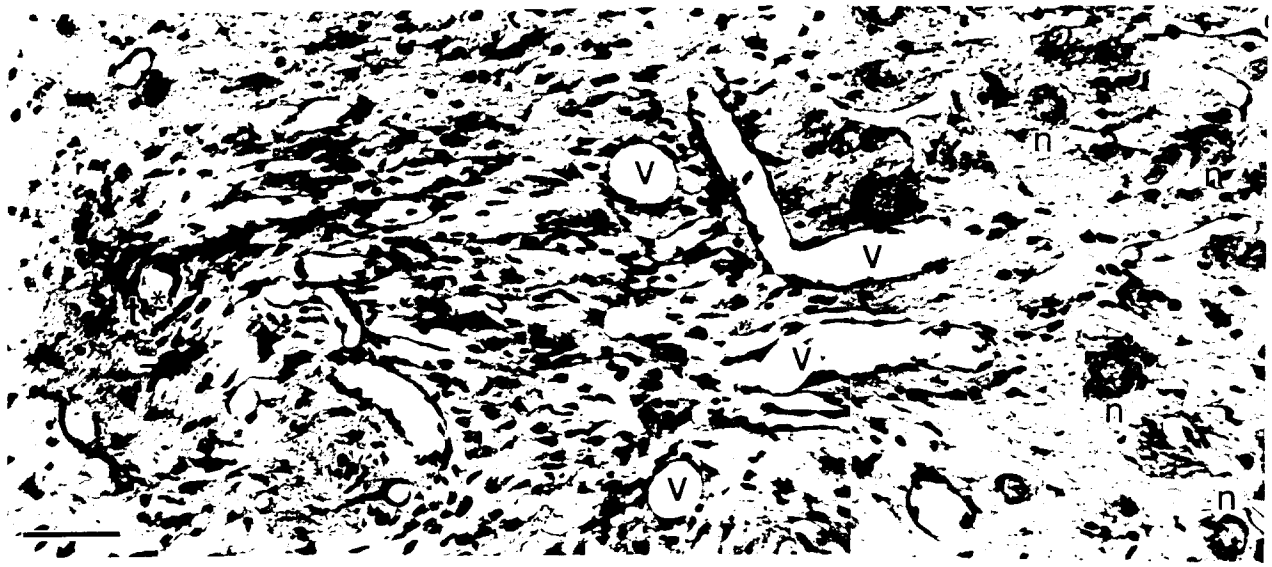

Figure 7. Sp99, H&E stain. The neurons (n) in the adjacent gray matter medial to the tip ($\overset{*}{t}$) of unpulsed electrode #3 appear normal. Note the glial scar and neovascularization (v) at the gray/white matter interface. Bar = 75 µm.

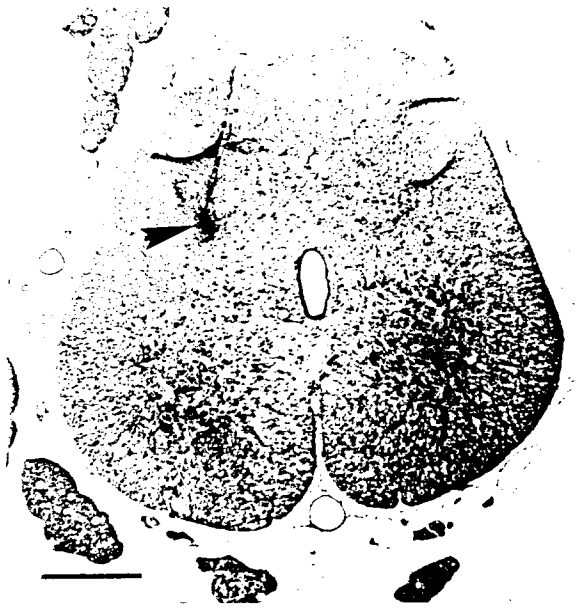

Figure 8. Sp100, H&E stain. A low magnification view of a section through the S_2 spinal cord shows the track of pulsed electrode #1. Note the dense deposit of India ink at the tip of this electrode (arrowhead). Bar = 750 µm.

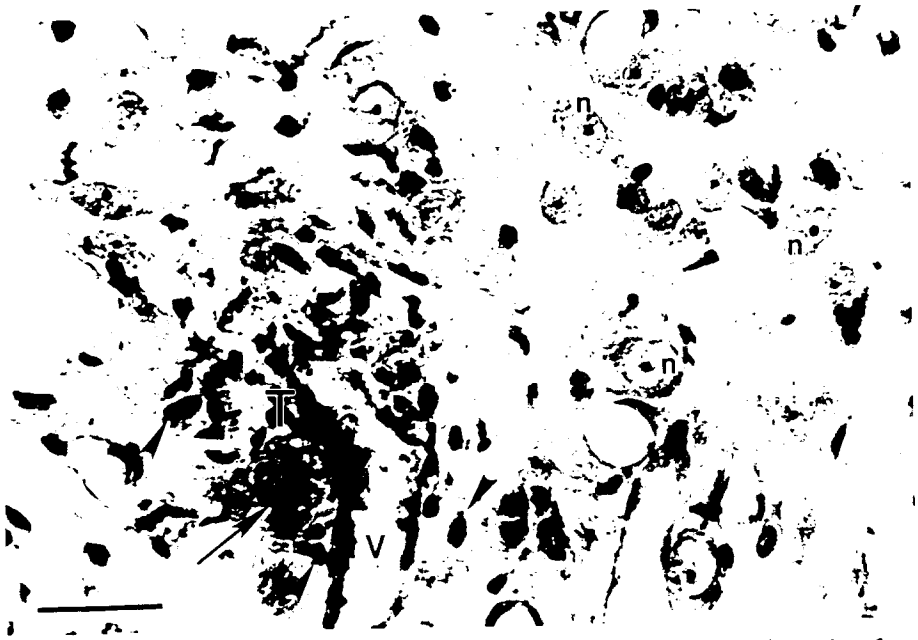

Figure 9. Sp100, H&E stain. Higher magnification through the sheath of pulsed electrode #, approximately 16 µm lateral to the site of the electrodes tip (T). Nearby neurons (n) appear to be normal. A few scattered lymphocytes (arrowheads) and a large debris-filled macrophage (arrow) are also shown near a blood vessel (v). Bar = 50 µm.

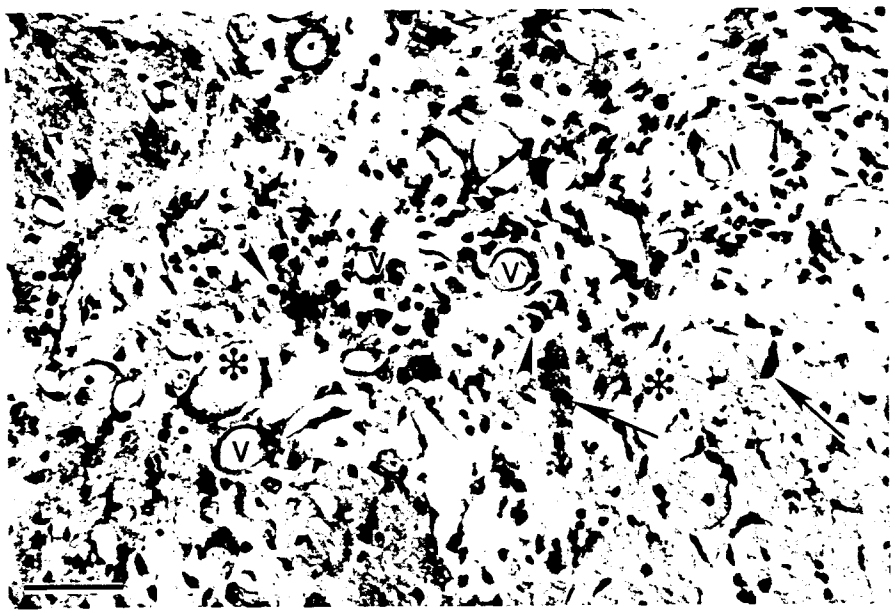

Figure 10. Sp100, Nissl stain. Tissue adjacent to the shaft of unpulsed electrode #2 contains a few lymphocytes (arrowheads), reactive astrocytes (arrows), neovascularization (v) and two neurons undergoing chromatolysis (*). Bar = 75 µm.

Figure 11. Sp100, Nissl stain. Higher magnification shows neuronal chromatolysis (*) approximately 50 µm from the shaft of unpulsed electrode #2. Bar = 15 µm.

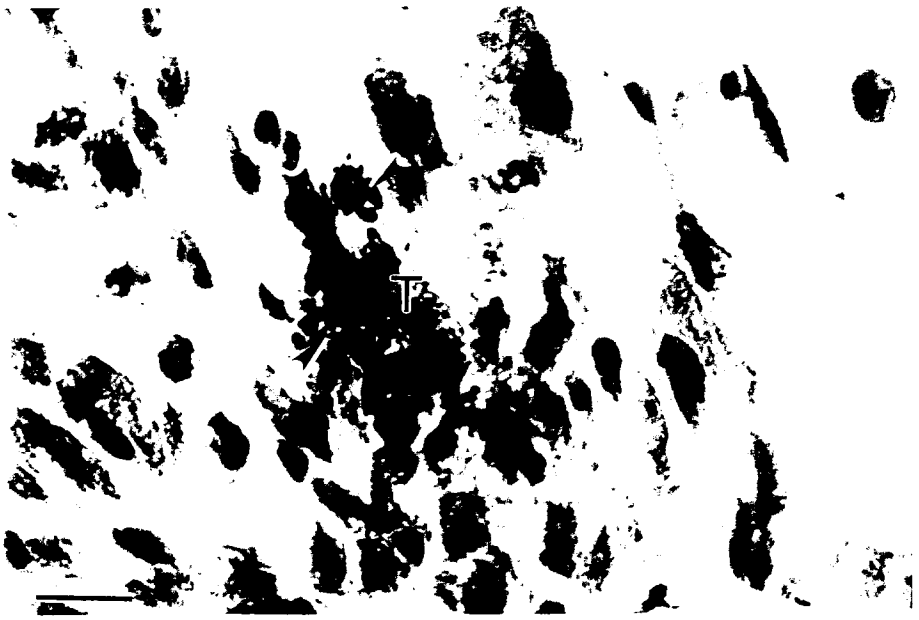

Figure 12. Sp100, H&E stain. Tissue near the tip (T) of unpulsed electrode #2 . The dark material represents cellular debris within phagocytes (arrowheads). Bar = 15 µm.

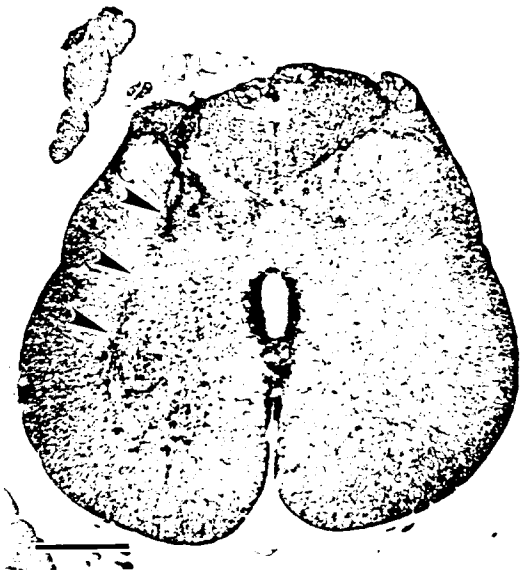

Figure 13. Sp100, GFAP (DAB) reaction, hematoxylin stain. Panorama of a section containing unpulsed electrode #2. Note the slightly darkened sector of the cord containing the electrode track (arrowheads). Bar = 750 µm.

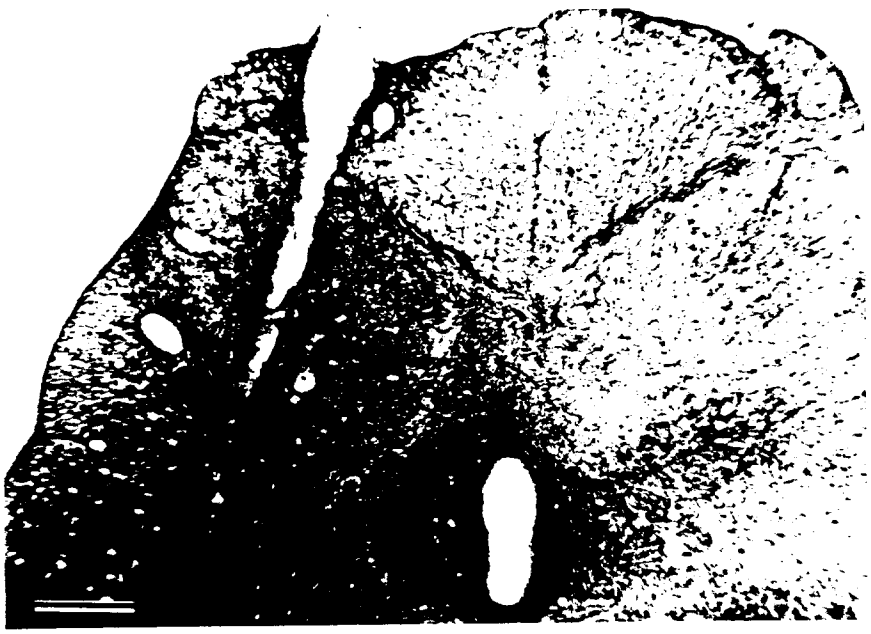

Figure 14. Sp100, GFAP (DAB) reaction, hematoxylin stain. Higher magnification of the ipsilateral side of the spinal cord shows a darkened region near the track of electrode #2. Bar = 375 µm.

Figure 15. Sp100, GFAP (DAB) reaction, hematoxylin stain. The tissue adjacent to the shaft of unpulsed electrode #2 (*) shows the densely stained reactive astrocytes (arrowheads) and their fibrous processes. Bar = 75 µm.

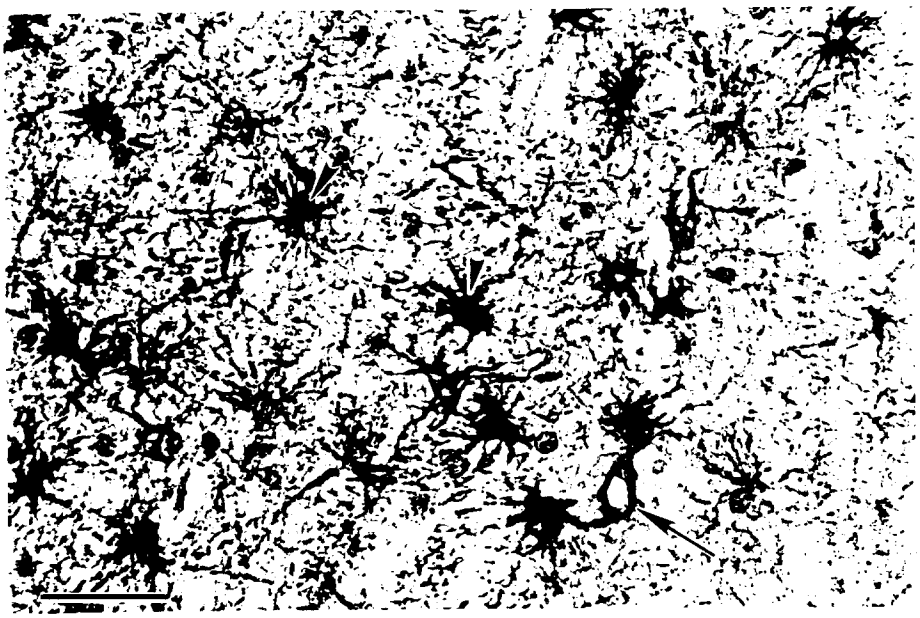

Figure 16. Cat cerebral cortex, GFAP (immunogold/silver enhanced) reaction, hematoxylin stain. Astrocytes and their processes are shown in this high magnification (arrowheads). Note the staining of the perivascular astrocytic end foot processes (arrow). Bar = 50 µm.

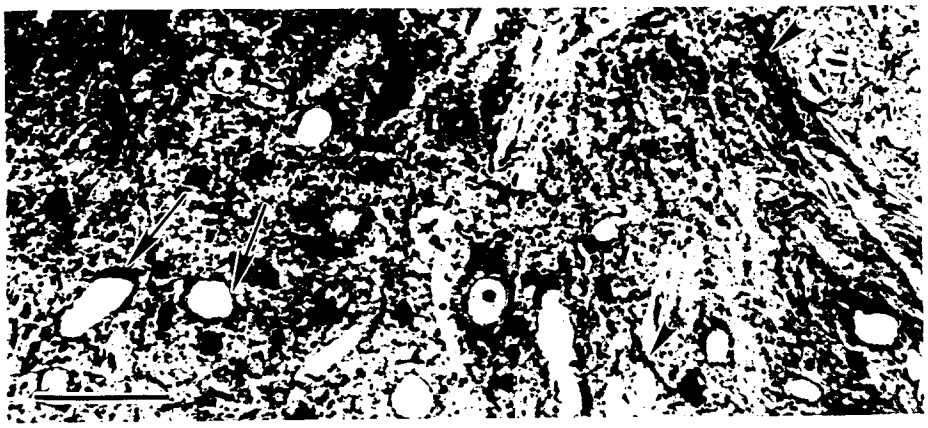

Figure 17. Sp86, GFAP (immunogold/silver enhanced) reaction, glycol methacrylate section, hematoxylin stain. This is a section of the cervical spinal cord from a previous animal perfused with IF. The border between the white (upper right corner) and gray matter is shown. Note the dense reaction product within astrocytic processes (arrowheads) and the perivascular staining (arrows). Bar = 50 µm.

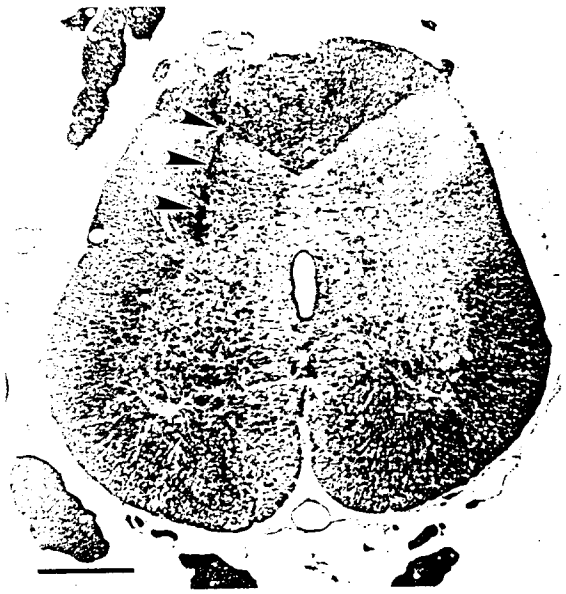

Figure 18. Sp100, NOS (DAB) reaction, hematoxylin stain. The track from pulsed electrode #1 shows a dark area (arrowheads). Bar = 750 µm.

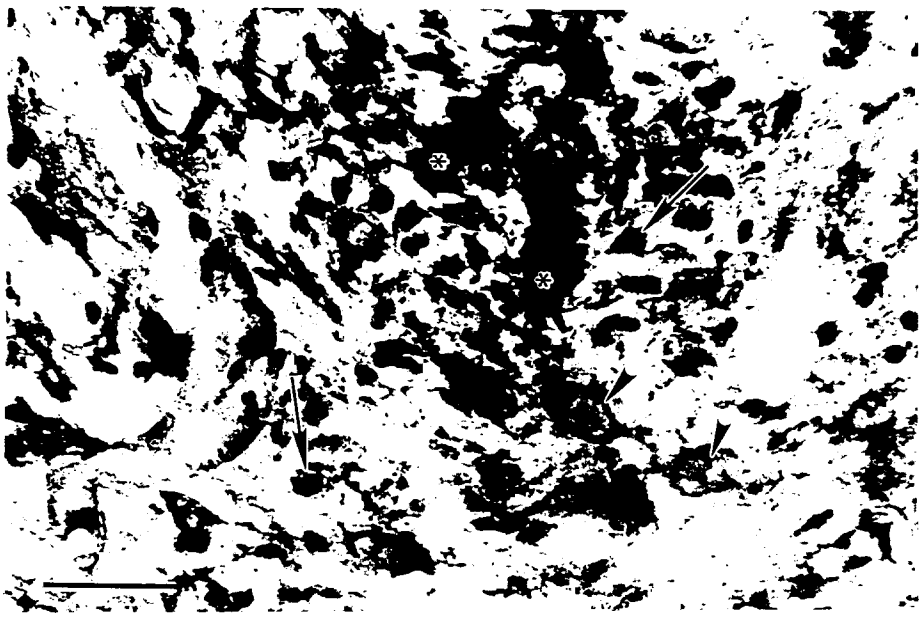

Figure 19. Sp100, NOS (DAB) reaction, hematoxylin stain. Higher magnification of the tip of pulsed electrode #1. Several cell types are stained, including neurons (arrowheads), and smaller cells, some of which are lymphocytes (arrows). The opaque material is India Ink (*). Bar = 50 µm.

Figure 20. Spinal cord from a cat perfused with IF, glycol methacrylate section, NOS (DAB) reaction, toluidine blue stain. This is a high magnification showing several stained neurons and their processes (arrowheads). These neurons appear brown against a blue background. Bar = 50 µm.

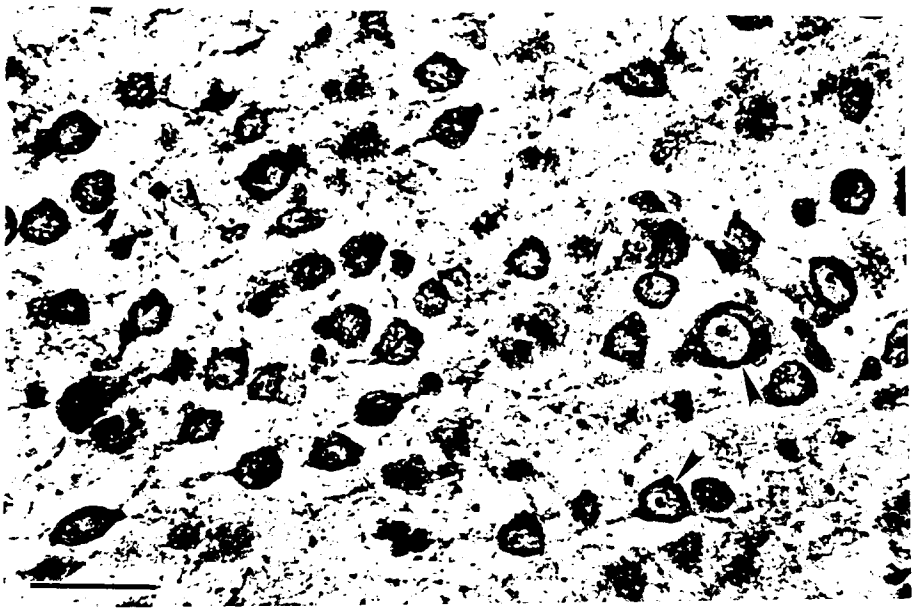

Figure 21. Cat cerebral cortex perfused with IF, NOS (DAB) reaction, osmium enhanced, hematoxylin stain. Note the stained neurons (arrowheads). Bar = 50 µm.

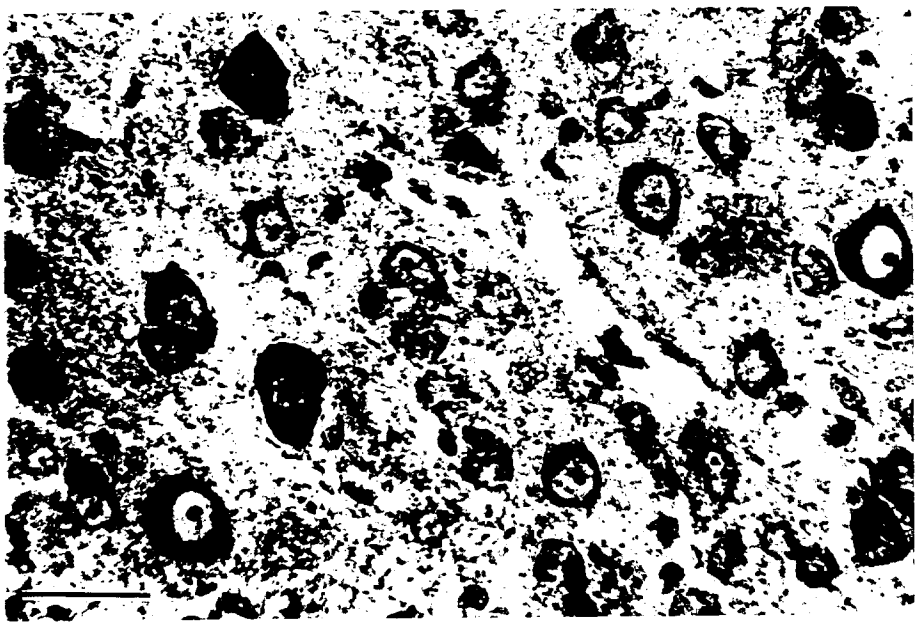

Figure 22. Cat cerebral cortex perfused with IF, GAP-43 (DAB) reaction, osmium enhanced, hematoxylin stain. Note the variable staining of these neurons. Bar = 50 µm.

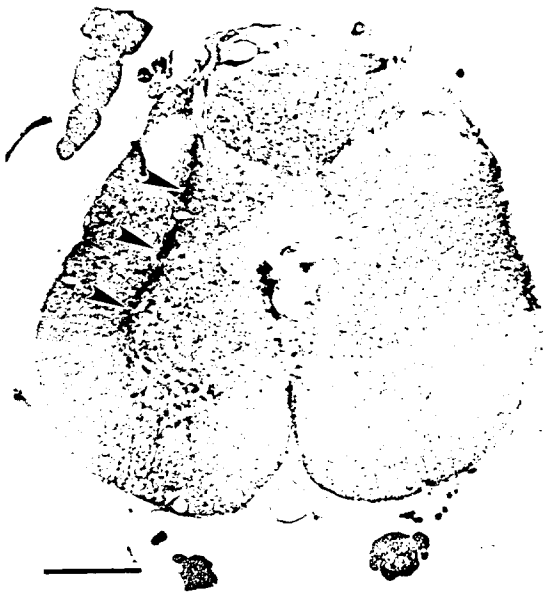

Figure 23. Sp100, ICAM-1 (DAB) reaction, hematoxylin stain. Panoramic view of a tissue section adjacent to the unpulsed electrode #3. The staining is localized primarily within the tissue surrounding the electrode track, and extending to the meningeal surface (arrowheads). Bar = 750 µm.

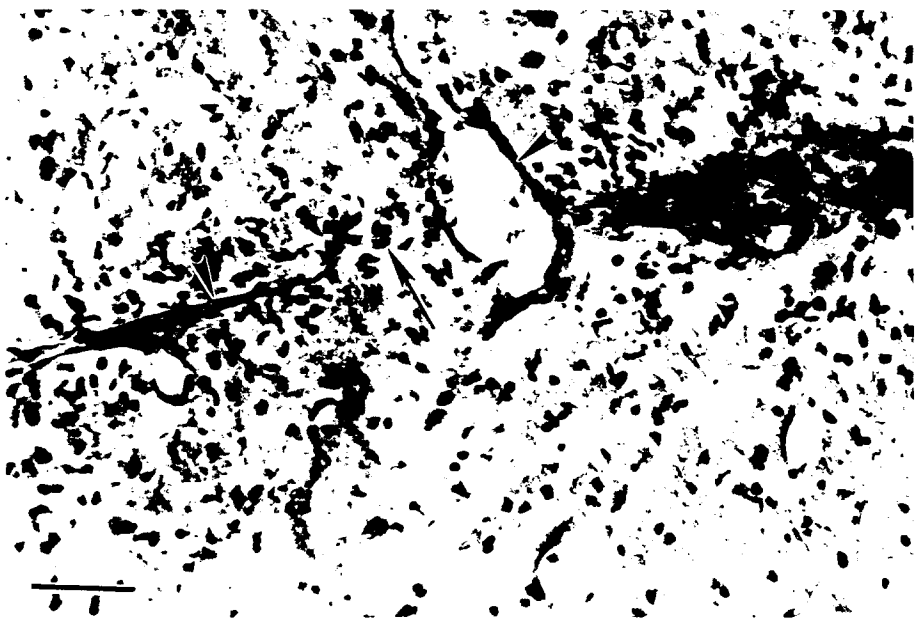

Figures 24, 25. Sp100, both figures ICAM-1 (DAB) reaction, hematoxylin stain. These two figures show at higher magnification the tracks of unpulsed electrode #3. Note the stained blood vessels (arrowheads), and some reactive cells (arrows). The Bar in Figure 24 = 75 µm

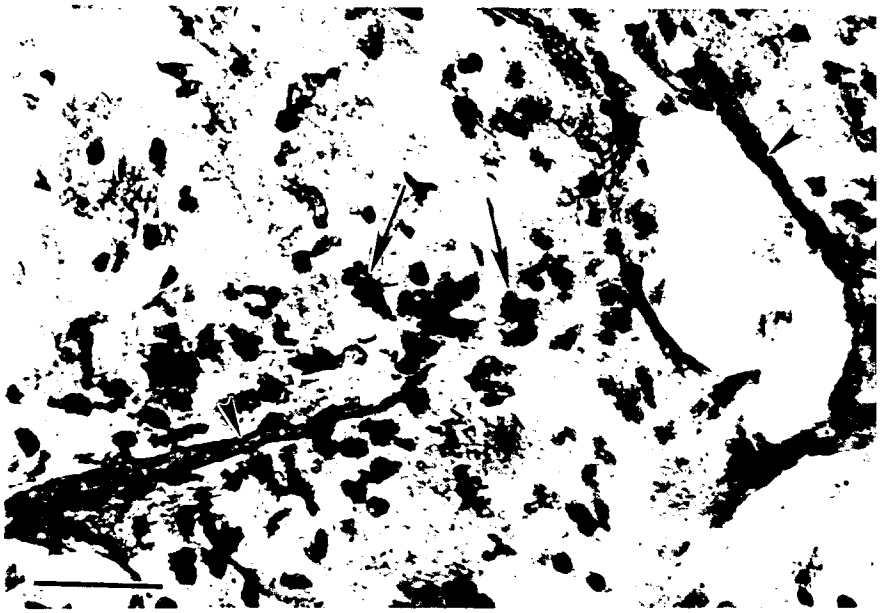

Figure 25. See legend for Figure 24. Bar = 50 µm.

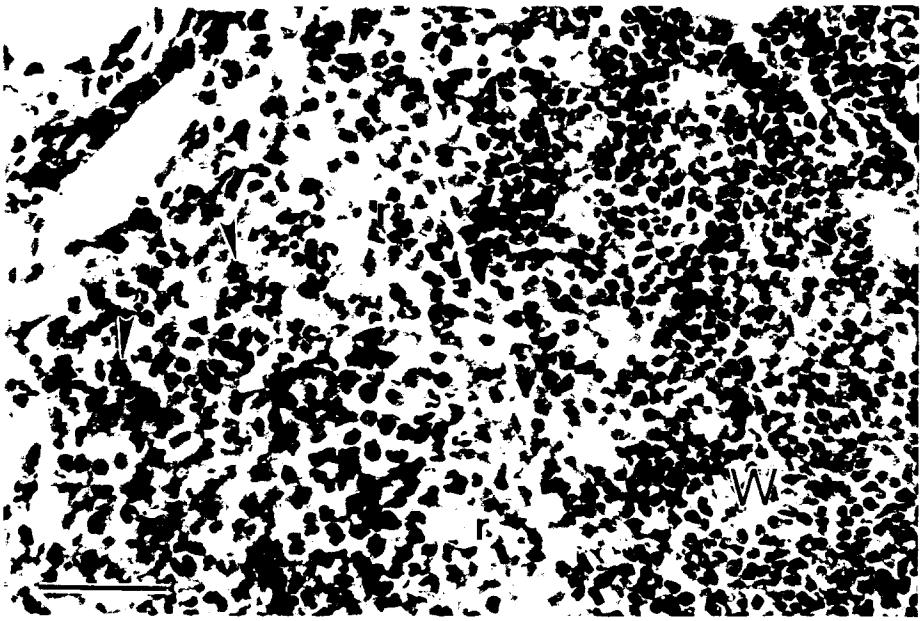

Figure 26. Spleen tissue from cat sp86 perfused with IF, CD13 (DAB) reaction, hematoxylin stain. Note the neutrophils darkly stained with the reaction product (arrowheads),. The stained cells are located primarily within the less densely packed red pulp (r), compared to the densely packed white pulp, containing mostly lymphocytes (w). Aggregates of neutrophils were stained brown against a blue background, while other mononuclear cells and lymphocytes did not stain brown. Bar = 50 µm.

Figures 27, 28. Representative negative controls for NOS and ICAM-1 in this series of immunohistochemistry experiments. Figure 27 is a paraffin section of cat cerebral cortex (H&E stain); Figure 28 is a glycol methacrylate section of cervical spinal cord from sp98 perfused with ½ K and stained with Toluidine blue. Note the absence of reaction product in any of the cell types. Bar Figure 27 = 150 µm.

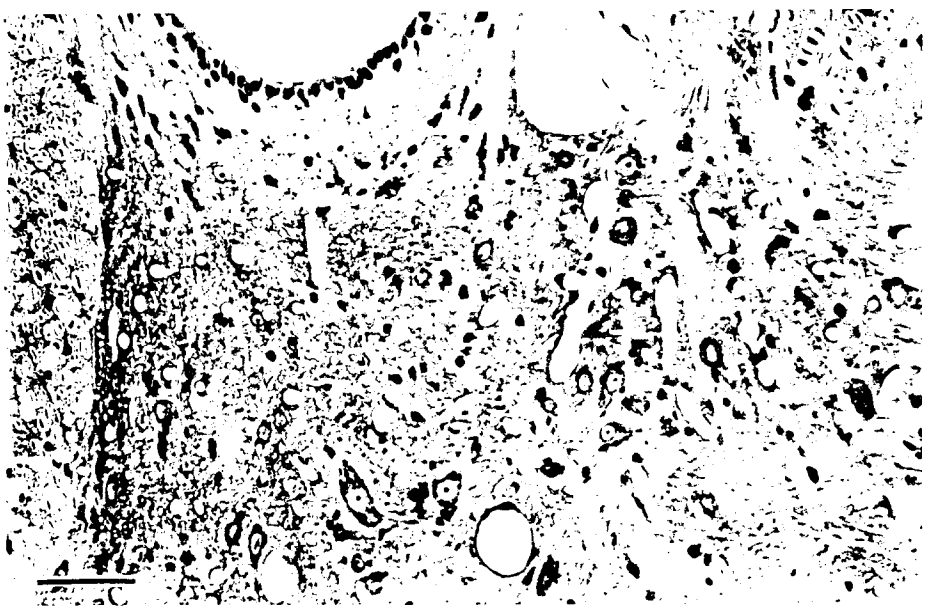

Fig. 28. See legend for Figs. 27, 28. Bar = 75 µm.